Anal. Chem. **2006,** *78,* 2623−2630

High-Performance, Static-Coated Silicon Microfabricated Columns for Gas Chromatography

Shaelah Reidy,† Gordon Lambertus,† Jennifer Reece,‡ and Richard Sacks*,†

Department of Chemistry, University of Michigan, Ann Arbor, Michigan 48109, and Department of Chemistry, Grinnell College, Grinnell, Iowa 50112

A procedure is described for the preparation of high-performance etched silicon columns for gas chromatography. Rectangular channels, 150 μm wide by 240 μm deep are fabricated in silicon substrates by gas-phase reactive ion etching. A 0.1−0.2-μm-thick film of dimethyl polysiloxane stationary phase is deposited on the channel walls by filling the channel with a dilute solution in 1:1 *n*-pentane and dichloromethane and pumping away the solvent. A thermally activated cross-linking agent is used for in situ cross-linking. A 3-m-long microfabricated column generated ∼12 500 theoretical plates at optimal operating conditions using air as carrier gas. A kinetic model for the efficiency of rectangular cross-section columns is used to evaluate column performance. Results indicate an additional source of gas-phase dispersion beyond longitudinal diffusion and nonequilibrium effects, probably resulting from numerous turns in the gas flow path through the channel. The columns are thermally stable to at least 180 °C using air carrier gas. Temperature programming is demonstrated for the boiling point range from *n*-C_5 to *n*-C_{12}. A 3.0-m-long column heated at 10 °C/min obtains a peak capacity of over 100 peaks with a resolution of 1.18 and a separation time of ∼500 s. With a 0.25-m-long column heated at 30 °C/min, a peak capacity of 28 peaks is obtained with a separation time of 150 s. Applications are shown for the analysis of air-phase petroleum hydrocarbons and the high-speed analysis of chemical warfare agent and explosive markers.

Several laboratories are working on the development of microfabricated columns for gas chromatography.[1−8] These columns are attractive because of their small size, low thermal mass allowing rapid temperature programming with relatively low power, and parallel manufacturing, which should result in low production costs. These attributes make these devices attractive for a number of applications involving on-site monitoring of environmental samples.

Most microfabricated column designs have used silicon microelectromechanical system (MEMS) technologies for column fabrication. Gas-phase reactive ion etching produces high-quality rectangular channels in silicon wafer substrates.[4,6,9−13] After etching, the open channels are sealed with Pyrex glass anodically bonded to the silicon surface. Back etching of the silicon substrate is used to remove excess substrate to further reduce thermal mass.[10] The high thermal conductivity of silicon allows for relatively uniform heating using spot heaters patterned on the back surface of the substrate.[10−12]

Several methods have been used for the deposition of a stationary phase on the silicon MEMS column walls. Most work has been done with nonpolar stationary phases such as dimethyl polysiloxane (PDMS).[14−16] The use of moderately polar trifluoropropylmethyl polysiloxane also has been reported.[14,15] Vapor

* Corresponding author. E-mail: rdsacks@umich.edu.
† University of Michigan.
‡ Grinnell College.

(1) Lorenselli, L.; Benvenuto, A.; Adami, A.; Guarnieri, V.; Margesin, B.; MUlloni, V.; Vincenzi, D. *Biosens. Bioelectron.* **2005**, *20*, 1968−1976.
(2) Bhushan, A.; Yemane, D.; Pasupuleti, P.; Overton, E. B.; Goettert, J.; Murphy, M. C. Fabrication and Testing of High Aspect Ratio Metal Micro-Gas Chromatograph Columns. Proc. ASME IMECE 2004, 2004 ASME International Mechanical Engineering Congress & Expo, Anaheim, CA, November 13−19, 2004.
(3) Bhushan, A.; Challa, V.; McKeon, J.; Yemane, D.; Overton, E. B.; Murphy, M. C.; Goettert, J. *TMS Lett.* **2004**, *1* (7), 145−146.
(4) Manginell, R. P.; Okandan, M.; Bauer, J. M.; Manley, R. G.; Trudell, D.; Kottenstette, R. J.; Lewis, P. R.; Adkins, D.; Heller, E. J.; Stewart, H.; Shul, R. J. *Micro Total Anal. Syst. 2004−μTAS '04* **2005**, *2* (297), 61−63.
(5) Overton, E. B.; Carney, K. R.; Roques, N.; Dharmasena, H. P. *Field Anal. Chem. Technol.* **2001**, *5* (1−2), 97.
(6) Yu, C. M.; Lucas, M.; Koo, C.; Stratton, P.; DeLima, T.; Behymer, E. *Micro-Electro-Mechanical Systems (MEMS)* 1998; Vol. 66, p 481.
(7) Noh, H.; Hesketh, P. J.; Frye-Mason, G. C. *J. Microelectromech. Syst.* **2002**, *11* (6), 718.
(8) Kolesar, E. D.; Reston, R. R. *IEEE Trans. Compon. Packag. Manuf. Technol.* **1998**, *21* (4), 324.
(9) Potkay, J. A.; Driscoll, J. A.; Agah, M.; Sacks, R. D.; Wise, K. D. Proc. 16th Annual IEE Conference on Micro-Electro-Mechanical Systems (MEMS), Kyoto, Japan, January 19−22, 2003; p 395.
(10) Agah, M.; Potkay, J.; Elstro, A.; Lambertus, G.; Sacks, R.; Wise, K. A. High-performance temperature-programmed gas chromatography column. North American Solid-State Sensors, Actuators, and Microsystems Workshop, Hilton Head Island, SC, June 6−10, 2004; pp 302−305.
(11) Agah, M.; Potkay, J. A.; Driscoll, J. A.; Sacks, R. D.; Kaviany, M.; Wise, K. D. Thermal Behavior of High-Performance Temperature-Programmed Microfabricated Gas Chromatography Columns. Technical Digest of the 12th International Conference on Solid-State Sensors, Actuators and Microsystems, Boston, MA, June 8−12, 2003; pp 1339−1342.
(12) Agah, M.; Potkay, J. A.; Lambertus, G. R.; Sacks, R. D.; Wise, K. D. *IEEE J. Microelectromech. Syst.* **2005**, *14* (5), 1039−1050.
(13) Zellers, E. T.; Steinecker, W. H.; Lambertus, G. R.; Agah, M.; Lu, C.-J.; Chan, H. K. L.; Potkay, J. A.; Oborny, M. C.; Nichols, J. M.; Astle, A.; Kim, H. S.; Rowe, M. P.; Kim, J.; Da Silva, L. W.; Zheng, J.; Whiting, J. J.; Sacks, R. D.; Pang, S. W.; Kaviany, M.; Bergstrom, P. L.; Matzger, A. J.; Kurdak, Ç.; Bernal, L. P.; Najafi, K.; Wise, K. D. A versatile MEMS gas chromatograph for environmental vapor mixture analysis. (Invited) Proceedings Solid-State Sensor, Actuator, and Microsystems Workshop, Hilton Head Island, SC, June 6−10, 2004; pp 61−66.

10.1021/ac051846u CCC: $33.50
Published on Web 03/14/2006

deposition prior to sealing the channel has been used,[17] but this restricts the upper temperature limit for further wafer processing to the upper temperature limit of the stationary phase. After the channel is sealed, stationary-phase application is usually performed by liquid coating means.

Static coating and dynamic coating are the two most frequently used methods for the production of wall-coated open-tubular fused-silica columns.[18] With dynamic coating, a plug of stationary phase in a suitable solvent is pushed through the column by the flow of a nonreactive gas. Stationary-phase film thickness can be controlled by means of the plug velocity and the stationary-phase concentration in the solvent. After the plug is expelled from the end of the column, the excess solvent is evaporated by continued gas flow leaving behind a film of stationary phase on the wall of the fused-silica tube. There are numerous variations on this general approach.[18]

For static coating, the entire column is filled with the stationary-phase solution, one end is sealed, and a vacuum applied to the open end. A front representing the liquid−vapor transition point propagates through the column away from the low-pressure end. The coating is complete once the solvent is completely pumped away. Static coating usually is preferred over dynamic coating for two reasons. First, all of the stationary phase initially introduced is deposited on the column wall; thus, the calculation of average film thickness is straightforward, using the surface area of the column, the concentration of stationary phase in the solution, and the density of the stationary phase. Second, the stationary-phase coating may be more uniform than with dynamic coating due to the lack of axial motion of the stationary phase during deposition.

Glass on silicon columns produced as part of the Engineering Research Center for Wireless Integrated Micro Systems (WIMS) at the University of Michigan has previously used dynamic coating for stationary-phase application. The columns are formed as 150 μm wide by 240 μm deep channels etched in 1 mm thick by 4 in. diameter silicon wafers. Columns with lengths of 0.25, 0.5, 1.0, and 3.0 m have been fabricated. Dynamic coating of PDMS has yielded columns with typically 2000−2500 theoretical plates/m.

Initial attempts at static coating of these silicon on glass columns failed due to bubble formation at the point where the round fused-silica connecting lines joined with the rectangular silicon channel. This occurred even after thorough degassing of the solvent.[18] This may be the result of cavitation in the liquid when the vacuum is applied. Recent work has solved these problems, and this report describes the coating and evaluation of silicon on glass columns with PDMS stationary phase applied by using static coating methods. Coatings in the 0.1−0.2-μm-thickness range are explored. Applications are emphasized where on-site, high-speed separations would be useful.

EXPERIMENTAL SECTION

Apparatus. Most experiments were conducted using the oven of a Varian 3500 conventional GC to ensure accurate temperature control. Commercial split/splitless inlets for an HP 6890 GC and flame ionization detectors (FID) from a Varian 3500 GC were used for all experiments. The Varian FID was used because it was easier to connect to alternative electrometer/amplifiers designed in-house for faster data logging. Data were logged with a sampling rate of 100 Hz. Some experiments were conducted at room temperature without a GC oven. For these experiments, a stand-alone HP 6890 inlet and Varian FID were used.

Table 1. Critical Dimensions of Microfabricated Columns

column length (cm)	chip dimensions (cm)	volume (cm^3)	surface area (cm^2)	no. of turns
25	1.1 × 1.1	0.009	1.95	70
50	1.5 × 1.5	0.018	3.9	102
100	1.9 × 1.9	0.036	7.8	142
300	3.2 × 3.2	0.108	23.4	230

Column Production and Coating. Column design and properties have been described in detail.[9−12] Briefly, the columns were produced in standard 4-in. silicon wafers by deep reactive ion etching using a modified Bosch process.[9−12] The rectangular cross-section channels, 150 μm wide by 240 μm deep, are etched as a double square spiral to accommodate a square chip format while utilizing chip surface area. Ports, 350 μm wide by 250 μm deep, were etched at opposite corners of each column, to accommodate fused-silica connection lines. After etching, the open surface of the wafer was sealed by anodically bonding a Pyrex glass wafer to the top surface of the silicon wafer. Conditions have been described.[9−12] After sealing, the wafers were diced into the individual columns.

Columns of four different lengths were fabricated. Critical dimensions are summarized in Table 1. Parallel processing is one of the potential advantages of microfabricated columns. For the 3.0-m-long columns, four were simultaneously etched on a single wafer. For the shorter columns, all three sizes were fabricated on a single wafer (nine 0.25 m, ten 0.50 m, and six 1.0 m). After dicing, 245-μm-o.d., 100-μm-i.d. deactivated fused-silica tubing (Polymicro Technologies, Pheonix, AZ) was connected to the etched ports by means of an epoxy seal (Hysol Epoxy Patch 1C, Rocky Hill, CT). Figure 1 shows a photograph of the completed columns illustrating the four column lengths. A coin is shown for size comparison.

Previous work with 3.0-m-long columns of similar design used a dynamic coating procedure, and these columns typically generated 2000−2500 theoretical plates/m.[14−16] Coating thickness was estimated at 1−2 μm. Static coating allows for more accurate estimation of film thickness and generates thinner, more uniform films.[18] Figure 2 shows the apparatus used for static coating of these microfabricated columns. Typically, coating solutions were prepared to give coating thickness in the range 0.1−0.2 μm. About 0.008 g of nonpolar dimethyl polysiloxane (OV-1, Ohio Valley, Specialty Chemical, Marietla, OH) was dissolved in 2.0 mL of a 1:1 (v/v) mixture of *n*-pentane and dichloromethane. The mixture was agitated for 30 min to ensure complete dissolution. After the columns were leak tested, they were filled completely with coating solution by using house nitrogen at a pressure of 24 psig at the solvent reservoir, which was connected to the column inlet by means of a segment of 250-μm-i.d. deactivated fused-silica tubing.

(14) Lambertus, G. R.; Elstro, A.; Sensenig, K.; Potkay, J.; Agah, M.; Scheuering, S.; Wise, K. D.; Dorman, F.; Sacks, R. *Anal. Chem.* **2004**, *76*, 2629.
(15) Lambertus, G. R.; Sacks, R. *Anal. Chem.* **2005**, *77*, 2078.
(16) Lambertus, G. R.; Fix, C. S.; Reidy, S. M.; Miller, R.; Wheeler, D.; Nazarov, E.; Sacks, R. D. *Anal. Chem.* In press.
(17) Lehmann, U.; Krusemark, O.; Müller, A.; Vogel, A.; Binz, P.; Krippner, P.; Schmidt, C. J. *Sensor* **2001**, *2*, 487−492.
(18) Grob, K. *Making and Manipulating Capillary Columns for Gas Chromatography*; Dr. Alfred Huthig Verlag: Heidelberg, 1986.

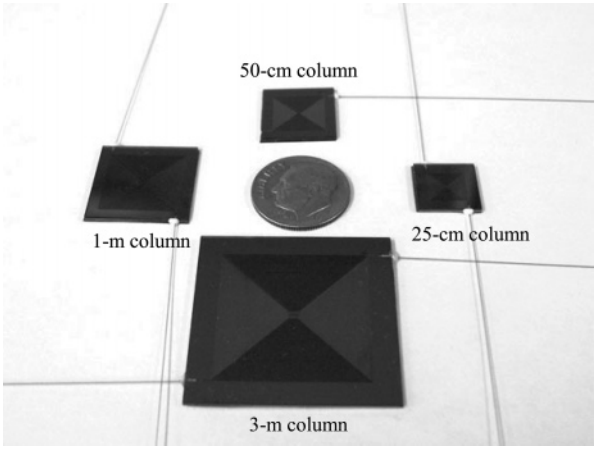

Figure 1. Photograph of silicon on glass microfabricated columns.

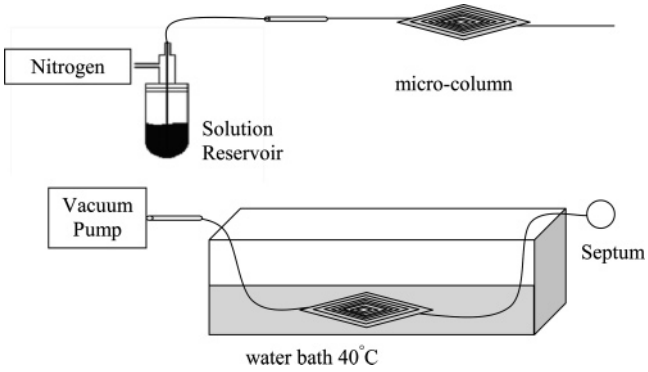

Figure 2. System used for static coating of silicon MEMS columns. Top shows filling configuration, and bottom shows solvent removal configuration.

After filling, the open end of the fused-silica connecting line was sealed by forcing it into a conventional GC septum. The column was then placed in a 40 °C water bath for 1 min, the house nitrogen turned off, and the reservoir disconnected. The open end was then connected to a vacuum pump (model UN 85.3 KTI, Newberger, Inc., Trenton, NJ) by means of a segment of 530-μm-i.d. deactivated fused-silica tubing. The solvent was evaporated at a pressure of ~3.25 psia until the column appeared empty (~15 min for a 1.0-m-long column). The column remained under vacuum in the water bath for an additional 2 h to ensure complete evaporation of the solvent.

Preliminary studies with static-coated silicon MEMS columns showed that even modest heating (80−100 °C) resulted in loss or degradation of the stationary phase. To stabilize the stationary phase for temperature-programmed applications, in situ cross-linking was used. Prior to coating, a thermally activated cross-linking agent[18] (dicumyl peroxide, 1 wt % nominal; Aldrich, Milwaukee, WI) was added to the liquid polymer phase. After coating, the column was heated to 180 °C at 5 °C/min and held at 180 °C for 4 h under nitrogen flow.

Materials and Procedures. Test mixtures were prepared using reagent-grade chemicals (Aldrich, Milwaukee, WI). Table 2 lists the compounds and their boiling points used for column evaluation. House air is used as carrier gas after purification for removal of water vapor and traces of organic compounds. Data acquisition from the FID is provided with a 16-bit A/D board (model DAS 1602-16, Computer Boards, Inc. Middleboro, MA) interfaced to a PC (Dell Dimension 8400). Interface control is provided by LabTech Notebook software (Version 10.1, Laboratory Technologies, Corp., Andover, MA). Column efficiency and flow calculations are made with Microsoft Excel spreadsheets. Chromatograms were processed with Grams/32 software (Galactic Industries, Salem, NH).

RESULTS AND DISCUSSION

Column Efficiency. Previous studies with columns of the same design as described here and with a nonpolar dimethyl polysiloxane stationary phase used dynamic coating and typically produced 2000−2500 theoretical plates/m.[14−16] With dynamic coating, the film thickness could not be directly determined but was assumed to be relatively thick (1−2 μm) based on the viscosity of the coating solution.[14] These relatively thick stationary-phase films are useful for increasing retention of very volatile target compounds, but under these conditions, resistance to mass transfer in the stationary phase makes a large contribution to overall peak variance. In addition, because the film thickness is unknown, it is difficult to quantitatively model the kinetic performance of the column.

The much thinner films and easily calculated film thickness provided by static coating offers the possibility of using a kinetic model to describe column efficiency. Several kinetic models that predict the dispersion of chromatographic bands in square and rectangular channels have been described. When Golay presented his classic kinetic model for the efficiency of wall-coated open-tubular columns, he also provided a theory for square columns.[19] He later extended the model for the case of rectangular columns[20] by developing a complex expression for gas flow through a rectangular column. Giddings et al.[21] developed a similar model for rectangular cross-section columns, which they called open parallel plate columns, but their expression for nonequilibrium effects in the moving phase considered only binary diffusion normal to the parallel plates.

Spangler[22,23] developed a kinetic model that addresses the efficiency of both rectangular and square cross-section channels. It considers binary diffusion in all directions for the calculation of nonequilibrium band broadening in the moving phase and thus takes into account the aspect ratio of the rectangular channel. A complex expression for average carrier gas velocity is derived and greatly simplified for the case of high aspect ratio (>5) rectangular channels. This expression was compared with literature values of gas velocity with excellent results.[23]

The work reported here is for a micro-GC column using silicon-based technologies, and Si chip size is an important consideration for a highly miniaturized, very-low-power instrument. High aspect ratio columns have been made in silicon wafers by the use of a relatively shallow etch (less than 50 μm) and a channel width of several tenths of millimeters.[23−24] For the present system, deep

(19) Golay, M. J. E. In *Gas Chromatography*; Coates, V. J., Noebels, H. J., Fagerson, I. S., Eds.; Academic Press: New York, 1958; pp 1−13 (East Lansing Symposium).
(20) Golay, M. J. E. *J Chromatogr.* **1981**, *216*, 1.
(21) Giddings, J. C.; Chang, J. P.; Myers, M. N.; Davis, J. M.; Caldwell, K. D. *J Chromatogr.* **1983**, *255*, 359.
(22) Spangler, G. E. Technical Proceedingsof the Third International Conference on Modeling and Simulation of Microsystems, San Diego, CA, March 2000; pp 562−565.
(23) Spangler, G. E. *J. Microcolumn Sep.* **2001**, *13* (7), 285.
(24) Kolesar, E. S.; Reston, R. R. *Surf. Coat. Technol.* **1994**, *68/69*, 679.

Table 2. Component List for Isothermal and Application Chromatograms

no.	compound	bp (°C)	no.	compound	bp (°C)
		Isothermal Chromatograms			
1	pentane	36.1	9	1-chloropentane	107
2	dichloromethane	39.8	10	toluene	110.6
3	2-butanone	79.6	11	2-fluorotoluene	113
4	ethyl acetate	77.1	12	cycloheptane	118.4
5	1,1,1-trichloroethane	74.1	13	octane	126
6	benzene	80.1	14	butyl acetate	126.1
7	2-pentanone	103.3	15	chlorobenzene	130
8	heptane	98.4			
		(a) Applications Chromatograms			
1	isopentane	30	13	*p*-xylene	138.3
2	methyl *tert*-butyl ether	55.2	14	*o*-xylene	144
3	hexane	69	15	nonane	150.8
4	benzene	80.1	16 17 18 19	isopropylbenzene	151
5	cyclohexane	80.7		1-metyhl-3-ethylbenzene	158
6	2,3-dimethylpentane	90		mesitylene	165
7	heptane	98.4		decane	174.1
8	toluene	110.6	20	1,2,3-trimethylbenzene	175
9	octane	126	21	*p*-isopropyltoluene	177
10	ethylbenzene	136.2	22	butylcyclohexane	181
11	2,3-dimethylheptane	141	23	undecane	195.9
12	*m*-xylene	139	24	dodecane	216.3
		(b) Applications Chromatograms			
1	cyclohexanone	155	3	2-nitrotoluene	220
2	DMMP	181	4	methyl salicylate	224

reactive ion etching is used to produce a deeper, narrower channel to make better use of the chip surface area.

High aspect ratio columns were not used for this study, and both the Golay and Spangler models[20] for rectangular cross-section columns were chosen as starting points for the evaluation of the static-coated columns. Equation 1 gives the kinetic model expression for rectangular cross-section open-tubular columns according to Golay.[20]

$$H = 2\frac{f_1 f_2 D_g}{u} + \frac{1 + 9k + \frac{51}{2}k^2}{105(1+k)^2}\frac{f_1 w^2}{f_2 D_g}u + \frac{2kd_f^2(w+h)^2}{3(1+k)^2 h^2 D_s}u \quad (1)$$

where H is the height equivalent to a theoretical plate, u is the average carrier gas velocity, k is the solute retention factor, d_f is the stationary-phase film thickness, D_g and D_s are the solute diffusion coefficients in the carrier gas (air) and the stationary phase, respectively, and w and h are width and height of the rectangular channel, respectively. In this equation, D_g is specified at the column outlet pressure, and f_1 and f_2 are Golay−Giddings and Martin−James gas compression corrections, respectively.

The first term on the right side of eq 1 describes band dispersion from longitudinal diffusion. The second term describes band dispersion from nonequilibrium effects in the gas phase, and the last term describes dispersion from nonequilibrium effects in the stationary phase. If w is at least 1000 times larger than d_f, the third term may be negligible for nonpolar silicone gum phases. Thus, for thin stationary-phase films, the critical parameter that impacts column efficiency is w^2/D_g. This term is proportional to the time required for solute molecules to diffuse from the center of the column to the column wall.

The average carrier gas velocity u for rectangular columns is obtained from eq 2.

$$u = \frac{w^2 p_o (P^2 - 1)}{24\eta L} f_2 \quad (2)$$

where p_o is the outlet pressure, P is the inlet-to-outlet pressure ratio, η is the carrier gas viscosity at the column temperature, and L is the column length.

Spangler presented a revised version of the Golay eq 3 to describe band dispersion in rectangular cross_section channels.[23]

$$H = 2\frac{f_1 f_2 D_g}{u} + \frac{0.9 + 2k + 35k^2}{96(k+1)^2}\frac{f_1 w^2}{f_2 D_g}u + \frac{2kd_f}{3(k+1)^2 D_s}u \quad (3)$$

Spangler's theory found the terms describing dispersion from longitudinal diffusion and nonequilibrium effects in the stationary phase to be identical to Golay's theory for round cross-section columns. The average linear carrier gas velocity equation and the dispersion term from nonequilibrium effects in the gas phase were revised. The coefficients in the second term were revised[23] from Golay.[19] Another notable difference is the omittance of an aspect ratio contribution by Spangler in the third term of the equation, which under high aspect ratios also drops from Golay's equation.

The average carrier gas velocity derived by Spangler[22] for rectangular cross-section columns is obtained from eq 4,

$$u = \frac{h^2 w^2 p_o (P^2 - 1)}{24\eta L(h^2 + w^2)} f_1 \quad (4)$$

where column dimensions play a larger role for low aspect ratios and converges with Golay's derivation for linear carrier gas velocities at high aspect ratios.

Plots 1 and 2 in Figure 3 show height equivalent to a theoretical plate versus average carrier gas velocity from eq 1 (Golay model)

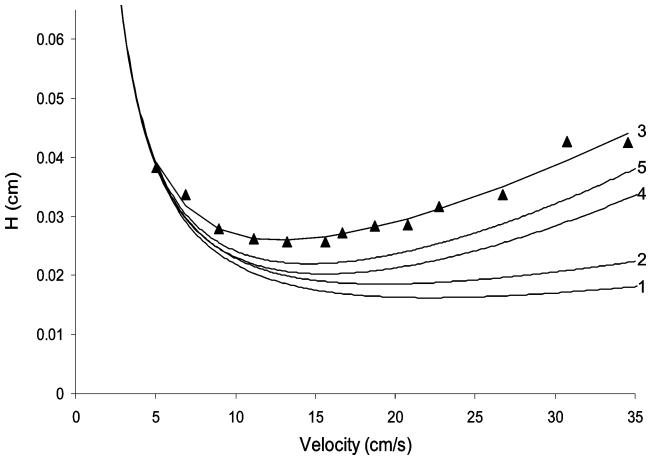

Figure 3. Height equivalent to a theoretical plate versus average carrier gas (air) velocity for a 3-m-long static-coated column. (1) plot from eq 1; (2) plot from eq 3; (3) plot for experimental data using *n*-octane at 40 °C; (4) and (5) plots 1 and 2 corrected for extracolumn band broadening using experimental data and eq 4, respectively.

and from eq 3 (Spangler model) for the conditions used in this study. The values of D_g and D_s were chosen as 0.093 [25] and 6.4 × 10^{-6} cm^2/s,[26] respectively. A k value of 2.5 and a viscosity of air (carrier gas) at 40 °C of 1.9 × 10^{-4} P [27] were used in the calculations. The column length was 3.0 m with channel width and depth of 150 and 240 μm, respectively. From plot 1, the minimum plate height is ~0.016 cm at an optimum carrier gas velocity of ~22 cm/s, while for plot 2, the minimum plate height is ~0.019 cm at an optimal carrier gas velocity of ~19 cm/s.

Plot 3 in Figure 3 shows experimental data of plate height versus average carrier gas velocity obtained for *n*-octane at 40 °C using the 3.0-m-long microfabricated column. The retention factor was 2.5 at this temperature. The minimum plate height is 0.025 cm, and the optimum carrier gas velocity is 14 cm/s. Note that the loss in column efficiency at the higher gas velocities is much more rapid and more nonlinear than predicted by eqs 1 and 3. This is characteristic of flow-dependent instrumental dead time and is not surprising considering the relatively short column used in this study. To evaluate this, the extracolumn band broadening term from eq 5 [28] was added to eqs 1 and 3.

$$H_{ec} = \frac{\Delta t^2}{L(k+1)^2} u^2 \qquad (5)$$

where H_{ec} is the height equivalent to a theoretical plate considering only extracolumn band broadening and Δt is the total instrumental dead time, which accounts for any dead time contributions from the inlet, connection lines, and the detector. Note that this source of band broadening increases as the square of the carrier gas velocity and thus can become very significant on the right-hand flanks of the Golay and Spangler plots.

The coefficient of u^2 in eq 5 was determined by fitting the experimental data in plot 3 of Figure 3 to the general form of the Golay equation given in eq 6

$$H = B/u + Cu + Du^2 \qquad (6)$$

The line shown in plot 3 of Figure 3 is the fit to eq 6. From the coefficient D and the known values of the column length and solute retention factor, the total instrumental dead time was found to be ~0.21 s for octane. Most of this can be attributed to the split inlet, the connecting lines, and the electrometer used to monitor the FID signal.

When this extracolumn band-broadening term is added to eqs 1 and 3, plots 4 and 5 in Figure 3 are obtained for the Golay and Spangler theories, respectively. The shapes of the plots and the plate height values are significantly closer to those of the experimental data in plot 3. The Spangler model proves to be a better fit to the experimental data, and thus, further consideration will only be given to this model. The minimum plate height from plot 5 is 0.022 cm, and the optimum carrier gas velocity is 15 cm/s.

From plot 3 in Figure 3, the 3.0-m-long column used in this study generates ~12 500 theoretical plates at the optimum carrier gas velocity. This is nearly 4200 plates/m and is substantially greater than the 2000−2500 plates/m typically generated with the dynamically coated columns previously described.[14−16] However, according to plot 5 in Figure 3, this column should be able to generate nearly 4700 plates/m when used with air carrier gas at the optimum operating velocity and with the experimental platform used in this study.

In Figure 4a, plot 5 from Figure 3 is resolved into its components based on the coefficients of the model described in eq 3 along with the extracolumn band-broadening term (D) from eq 6. Plot 5 from Figure 3 is also reproduced for reference (H_5). In Figure 4b, plot 3 from Figure 3 is resolved into its components based on the coefficients B, C, and D from eq 6. Plot 3 from Figure 3 is also reproduced for reference (H_3).

Plots labeled D, for extracolumn band broadening, in the two sets are identical since, in both cases, they are from fits to the experimental data of plate height versus average carrier gas velocity. Plots labeled B, for longitudinal diffusion, are quite similar for the two sets of plots, suggesting that the value of gas-phase binary diffusion coefficient used in the calculations (0.093 cm^2/s) is reasonably accurate. For plots C from nonequilibrium effects, both the gas-phase contribution C_g and the stationary-phase contribution C_s obtained from eq 3 are shown in Figure 4a. The sum of these is also shown in the figure. In Figure 4b, only the sum can be obtained from eq 6 using the fit to the experimental data.

Two things should be noted regarding the C terms. First, from Figure 4a, the C_s contribution is very small, typically contributing ~2.5% to the sum. This is the result of the thin stationary-phase films obtained from static coating. Second, the C-term sum is substantially larger in Figure 4b, and this is the main source of difference between the overall values of H for the model modified by the extracolumn band broadening (plot 5 in Figure 3) and the fit to the experimental data (plot 3 in Figure 3). It is not expected that pooling or sagging of the stationary phase in the 90° turns

(25) Fuller, E. N.; Schettler, P. D.; Giddings, J. C. *Ind. Eng. Chem.* **1966**, *58* (5), 19.
(26) Kong, J. M.; Hawkes, S. *J. J. Chromatogr. Sci.* **1976**, *14* (6), 279−287.
(27) Weast, R., Ed. *CRC, Handbook of Chemistry and Physics,* 49th ed.; The Chemical Rubber Co.: Cleveland, OH, 1968.
(28) Gaspar, G.; Annino, R. Vidal-Madjar, G.; Guiochon, G. *Anal. Chem.* **1978**, *50*, 1512.

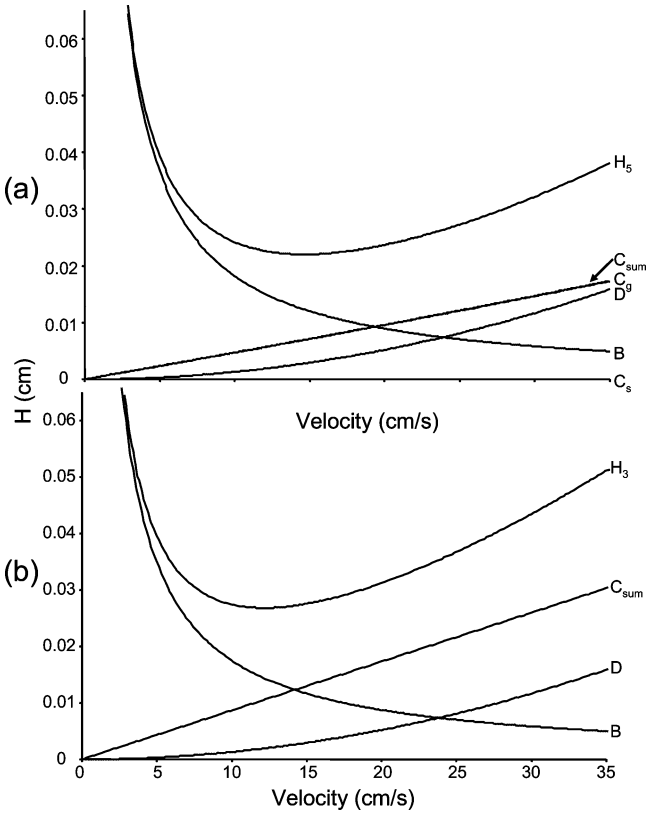

Figure 4. Height equivalent to a theoretical plate versus average carrier gas (air) velocity for a 3-m-long static-coated column showing plot 5 (a) and plot 3 (b) from Figure 3 resolved into the individual band-broadening sources. *B*, longitudinal diffusion; C_g, gas-phase nonequilibrium effects; C_s, stationary-phase nonequilibrium effects; *D*, extracolumn band broadening. In (a), the sum of C_g and C_s is shown. In (b), only the sum is shown.

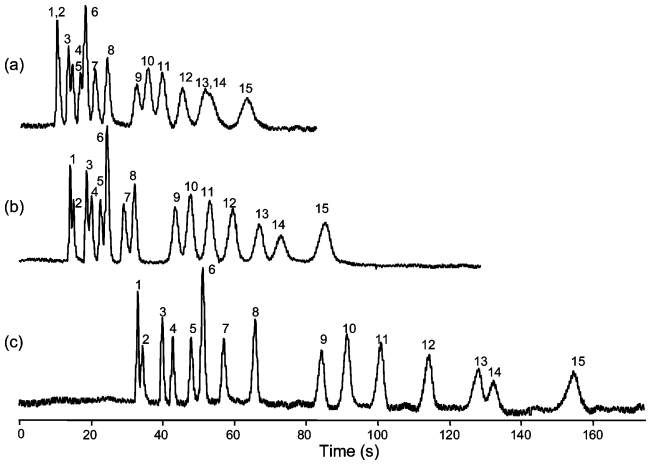

Figure 5. Test chromatograms of a 15-component mixture separated isothermally at 30 °C using a 0.5- (a), 1.0- (b), and 3.0-m-long static-coated columns. Peak numbers correspond to compound numbers in Table 2.

or down the column walls contributes significantly to band dispersion as a result of static coating. Even significant errors in the estimation of the stationary-phase diffusion coefficient or the channel dimensions are unlikely to change C_s enough to account for the difference in the sums. Thus, it is probable that the value of the C_g term accounts for the poorer efficiency of the microfabricated column relative to the predictions of the model.

These data suggest either a significant error in the channel width value used in computing the C_g term or an additional source of gas-phase band broadening not accounted for in eq 3. The columns used in this study make many sharp turns. For the 3-m-long column, a total of 230 right-angle turns are made, half left turns and half right turns. Studies with microcolumn liquid-phase separations[29−31] have shown that the so-called race track effect can cause significant dispersion in the moving phase. The point is that solute molecules on the outside of a turn travel further during the turn than molecules on the inside. Because of diffusion across the channel, having the same number of right and left turns does not completely cancel this added dispersion. Modeling of this source of band broadening for liquid-phase separations shows that, like the C_g term, dispersion increases with increasing moving-phase velocity and decreases with increasing moving-phase binary diffusion coefficient. This could explain the larger *C* term observed in the results from the experimental data relative to the value predicted from eq 3. Further work is in progress to clarify these points for microfabricated GC columns.

Test Chromatograms. Figure 5 shows chromatograms from a 15-component multifunctional test mixture using a 0.5- (a), a 1.0- (b), and a 3.0-m-long (c) static-coated microfabricated column. Properties of the columns are listed in Table 1. Peak numbers correspond to component numbers in Table 2 under isothermal chromatograms. The chromatograms were obtained at room temperature (24 °C) using a stand-alone split/splitless inlet and a stand-alone FID. The injection size was 0.1 μL, and the split ratio was 400:1. All columns were operated at their optimal flow rate (15−20 cm/s).

With all three columns, peak shapes are excellent with no signs of tailing or other artifacts. Since the stationary-phase film thickness is only ~0.15 μm, the lack of tailing suggests that the untreated silicon surface is not highly active for these components and, for many applications, may be directly coated without the need for prior deactivation.

Temperature-Programmed Operation. Previous studies with fused-silica capillary columns using air as the carrier gas showed that commercial columns with cross-linked dimethyl polysilxane could be heated to 210 °C for extended periods of time without degradation of the stationary phase.[32,33] Rapid degradation occurred at a temperature of 230 °C. The thermal stability of silicon MEMS columns with air carrier gas at elevated temperatures has not been studied. To reduce the risk of column degradation, temperature-programmed studies were limited to a maximum temperature of 180 °C.

Figure 6 shows temperature-programmed chromatograms of a *n*-C_5 to *n*-C_{12} normal alkane mixture using a 3.0- (a) and a 0.25-m-long column (b). Both columns were static-coated and cross-linked. The starting temperature was 30 °C and the programming rates were 30 (A), 20 (B), and 10°C/min (C) for the 3.0-m-long

(29) Fu, L.-M.; Yang, R.-J.; Lee, G.-B. *Electrophoresis* **2002**, *23*, 602−612.
(30) Molho, J. I.; Herr, A. E.; Mosier, B. P.; Santiago, J. G.; Kenny, T. W. *Anal. Chem.* **2001**, *73*, 1350−1360.
(31) Culbertson, C. T.; Jacobson, S. C.; Ramsey, J. M. *Anal. Chem.* **1998**, *70*, 3781−3789.
(32) Grall, A. J.; Sacks, R. D. *Anal. Chem.* **1999**, *71*, 5199.
(33) Grall, A. J.; Zellers, E. T.; Sacks, R. D. *Environ. Sci. Technol.* **2001**, *35*, 163.

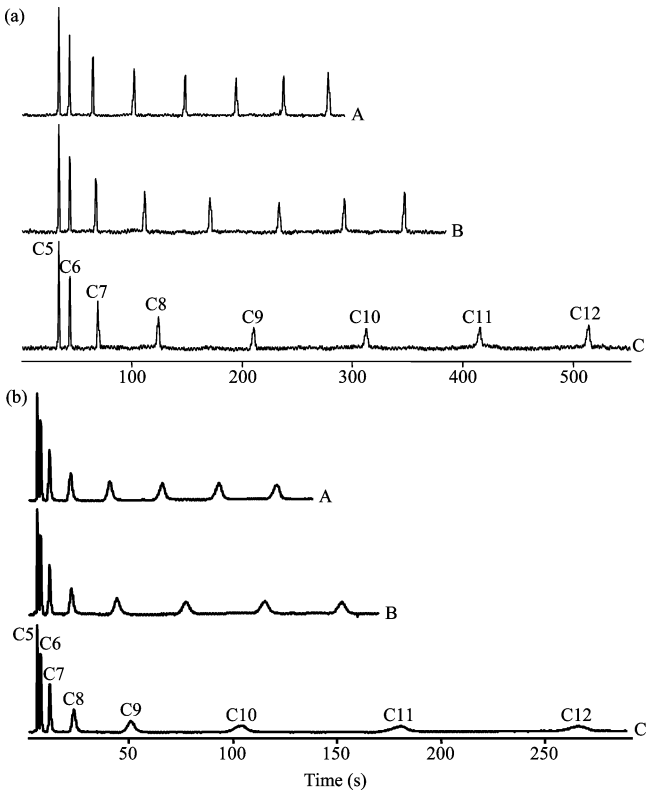

Figure 6. Temperature-programmed chromatograms of an *n*-C_5 to *n*-C_{12} mixture of normal alkanes using a 3.0- (a) and a 0.25-m-long column (b). For (a), programming rates were 30 (A), 20 (B), and 10 °C/min (C). For (b), the programming rates were 50 (A), 30 (B), and 10 °C/min (C). In all cases, the starting temperature was 30 °C and the final temperature was 180 °C.

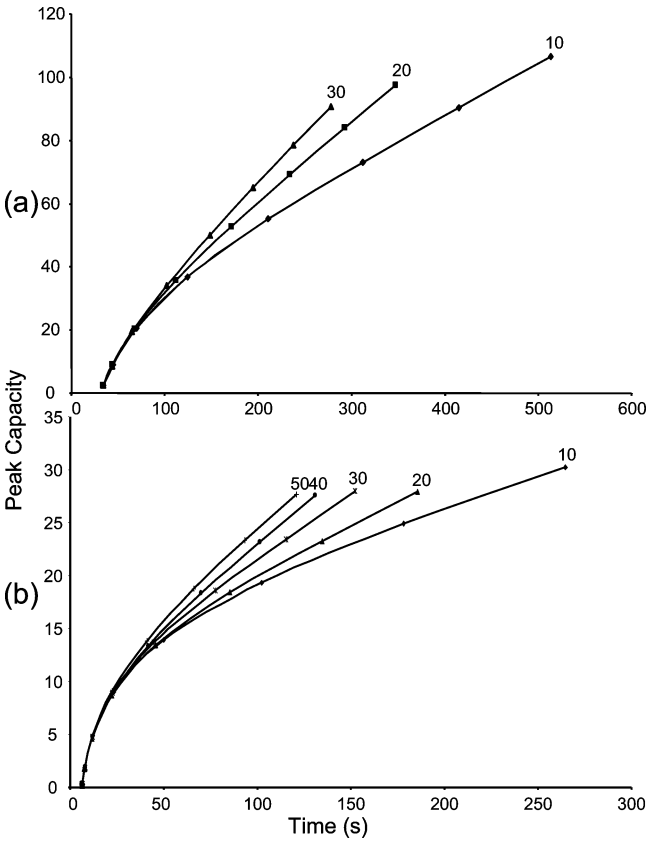

Figure 7. Cumulative peak capacity nc versus retention time for the temperature-programmed separation of a *n*-C_5 to *n*-C_{12} normal alkane mixture using a 3.0- (a) and a 0.25-m-long (b) static-coated column. Numbers next to plots give temperature-programming rates in °C/min. In all cases, the starting temperature was 30 °C and the final temperature was 180 °C.

column and 50 (A), 30 (B), and 10 °C/min (C) for the 0.25-m-long column. The 3- and 0.25-m-long columns were operated at 14 and 18 cm/s, respectively. Note that, with temperature programming, higher boiling point compounds benefit from on-column focusing, and the effects of extracolumn band broadening from the split inlet are reduced. This is particularly useful with the relatively short columns used in this study. No peak tailing or other artifacts are observed. With the shorter column and the 50 °C/min programming rate, *n*-C_{12} is eluted in ~120 s with a peak capacity of ~28 peaks.

Figure 7 shows plots of cumulative peak capacity n_c versus retention time obtained from the chromatograms shown in Figure 6. The cumulative peak capacity n_c (resolution 1.18) for the retention range *n*-C_x to *n*-C_y is obtained by summing the Trenzahl numbers (TZ) according to eqs 7 and 8 and adding the reference peaks.[34–37]

$$\mathrm{TZ} = \frac{t_{R(n+1)} - t_{R(n)}}{w_{1/2(n)} + w_{1/2(n+1)}} - 1 \qquad (7)$$

$$\mathrm{n}_c = \sum_{n=x}^{n=y} (\mathrm{TZ} + 1) \qquad (8)$$

where $t_{R(n)}$ and $t_{R(n+1)}$ are the retention times of two adjacent normal alkanes and $w_{1/2(n)}$ and $w_{1/2(n+1)}$ are the corresponding full widths at half-peak height. For example, with the 0.25-m-long column and a programming rate of 50 °C/min, *n*-C_{10} is eluted in ~70 s with a total peak capacity of 18 peaks. Note that with the 3.0-m-long column and a 10 °C/min programming rate the entire chromatogram has a peak capacity of ~105 peaks.

Previous work with temperature-programmed GC has shown that if the temperature change of the column is no more than ~15 °C during a time interval equal to the column holdup time, then the loss of peak capacity relative to lower programming rates is minimal.[38] For the 0.25-m-long column used in this study, the holdup time is ~2 s. This suggests that much higher programming rates than the 50 °C/min used here can be used with corresponding reductions in analysis time. However, 50 °C/min is about the highest rate that can be achieved with the commercial GC used in this study. This clearly shows the limitations of conventional conve ctive ovens for high-speed GC with short microfabricated columns.

Figure 8 shows temperature-programmed chromatograms of an air-phase petroleum hydrocarbon mixture (a) using a 3.0-m-long column and a mixture of chemical warfare agent markers (b) using a 0.25-m-long column. Mixture a is available com-

(34) Hurrell, R. A.; Perry, S. G. *Nature* **1962**, *196*, 571.
(35) Grob, K., Jr.; Grob, K. *J. Chromatogr.* **1981**, *207*, 291.
(36) Ettre, L. A. *Chromatographie* **1975**, *80*, 291.
(37) Kaiser, R. *Chromatographie in der Gas phase*, 2nd ed.; Bibliografisches Institut: Mannheim, Germany. 1966; Vol. 2.
(38) Grall, A.; Leonard, C.; Sacks, R. *Anal. Chem.* **2000**, *72*, 591.

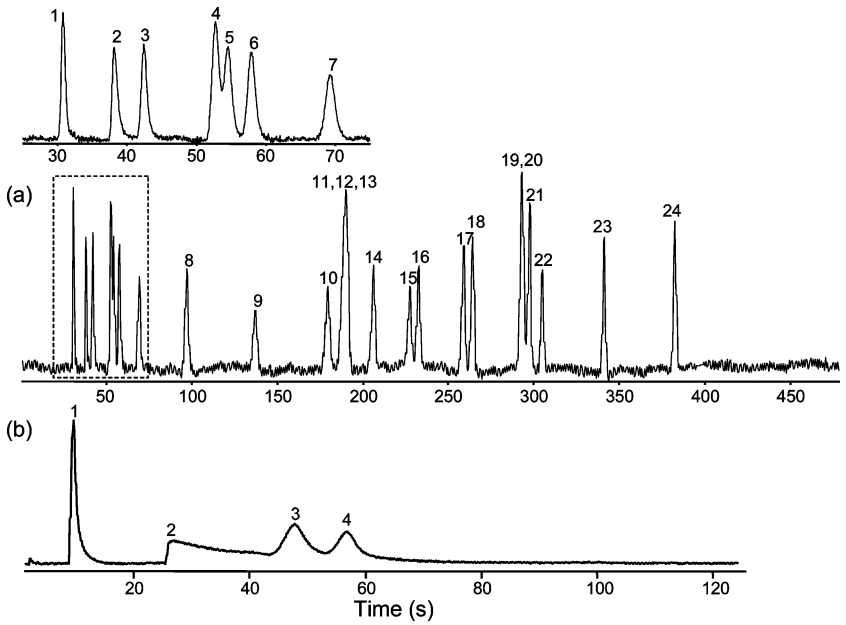

Figure 8. Temperature-programmed chromatograms of an air-phase petroleum hydrocarbon mixture (a) using a 3.0-m-long column and a mixture chemical warfare and explosive agent markers (b) using a 0.25-m-long column. Chromatogram a had an initial hold at 30 °C for 2 min and then ramped to 180 °C at 30 °C/min. Chromatogram b was ramped at 30 °C/min from 40 to 180 °C.

mercially and is used to monitor waste site remediation. For this mixture, the starting temperature was 30 °C, and after a 2.0-min isothermal hold, the column was heated at 30 °C/min to 180 °C with an average carrier gas velocity of ~14 cm/s. The inset above and to the left shows the early portion of the chromatogram on an expanded time scale. The peak shapes are excellent. Two coelutions are observed. Note that the two xylene isomers (peaks 12 and 13) are difficult to separate with any column. Note that under isothermal conditions the separation of components 19 and 20 can be improved. For chromatogram b, the programming rate was 30 °C/min. with a starting temperature of 40 °C with an average carrier gas velocity of ~12 cm/s. The chromatogram is complete in less than 1 min. Note that the very polar DMMP is severely tailed on the microfabricated column. This is potentially due to active sites on the column. Tailing is seen with many polar compounds though DMMP is most severe. Peak numbers correspond to compounds listed in Table 2, applications chromatograms a and b, respectively.

CONCLUSIONS

Static coated, thin-film silicon MEMS columns with in situ cross-linking have been prepared that can generate over 4000 theoretical plates/m. This compares favorably with commercial fused-silica wall-coated open-tubular columns. The cavitation problems experienced with earlier attempts at static coating appear to be solved, and column coating is relatively straightforward and rapid. It appears that the surface activity of the native etched silicon surface is sufficiently low that it can be wetted by a thin film of PDMS, and thus for many potential applications, no surface deactivation is necessary prior to coating. A 3.0-m-long column generates ~12 500 theoretical plates under isothermal conditions with air as carrier gas and a peak capacity of over 100 peaks for temperature-programmed separation at 10 °C/min of an *n*-C_5 to *n*-C_{12} alkane mixture.

With in situ cross-linking, these columns appear thermally stable to at least 180 °C using air carrier gas. The use of air is particularly attractive for on-site applications and for remote sensing where the need for on-board carrier gas supplies is a significant limitation. However, the optimum carrier gas velocities in air are significantly lower than with more diffusive gases such as hydrogen and helium. This results in longer separation times at a specified resolution. In addition, the upper temperature limit with air is significantly lower than with hydrogen or helium.

Column efficiency studies suggest that there is additional gas-phase band broadening occurring with these silicon MEMS columns beyond that usually associated with longitudinal diffusion and nonequilibrium effects. This may be attributed to the large number of turns in the gas flow path associated with the column geometry (race track effect). For the 3.0-m-long column evaluated in this study, this geometric dispersion appears comparable in magnitude to nonequilibrium effects in the gas phase. Further work is needed in this area.

ACKNOWLEDGMENT

The authors express their appreciation to Dr. Ken Wise, Mr. Masoud Agah, Mr. Joseph Potkay, and Ms. Katharine Beach at the University of Michigan Electrical Engineering and Computer Science Department for fabrication of the columns. Funding for this work was provided by the University of Michigan Center for Wireless Integrated Microsystems (WIMS) through the Engineering Research Centers Program of the National Science Foundation under Award ERC-9986866. Additional support is provided by Grant R01-OH03692 from the National Institute for Occupational Safety and Health of Centers for Disease Control and Prevention (NIOSH-CDCP).

Received for review October 14, 2005. Accepted January 30, 2006.

AC051846U